Supplementary Material (ESI) for Chemical Communications

Conformation Dynamics of non-, singly- and doubly-*N*-fused [28]hexaphyrins revealed by photophysical studies

Jong Min Lim,[a] Mitsunori Inoue,[b] Young Mo Sung,[a] Masaaki Suzuki,[b] Tomohiro Higashino,[b] Atsuhiro Osuka,[b]* and Dongho Kim[a]*

[a]*Spectroscopy Laboratory for Functional π-electronic Systems and Department of Chemistry, Yonsei University, Seoul 120-749, Korea*

[b]*Department of Chemisty, Graduate School of Science, Kyoto University, Sakyo-ku, Kyoto 606-8502, Japan.*

*To whom it may correspondence should be addressed.

E-mail: *dongho@yonsei.ac.kr*; *osuka@kuchem.kyoto-u.ac.jp*

1. Experimental Section

1-1. Steady-state absorption

Steady-state absorption spectra were obtained by using an UV/VIS/NIR spectrometer (Varian, Cary5000). Quartz cell with optical path length of 10 mm was used for all steady-state measurements. Solvents, chloroform, dichloroform, tetrahydrofuran, and toluene, were obtained from Sigma-Aldrich (spectroscopic grade) without further purification. The samples' absorption spectra were monitored during each experiment for changes arising from permanent photo bleaching and photochemical processes.

1-2. Femtosecond Transient Absorption Measurements

The femtosecond time-resolved transient absorption (TA) spectrometer consisted of homemade noncollinear optical parametric amplifier (NOPA) pumped by a Ti:sapphire regenerative amplifier system (Quantronix, Integra-C) operating at 1 kHz repetition rate and an optical detection system. The generated visible NOPA pulses had a pulse width of ~ 100 fs and an average power of 1 mW in the range 480-700 nm which were used as pump pulses. White light continuum (WLC) probe pulses were generated using a sapphire window (2 mm of thickness) by focusing of small portion of the fundamental 800 nm pulses which was picked off by a quartz plate before entering to the NOPA. The time delay between pump and probe beams was carefully controlled by making the pump beam travel along a variable optical delay (Newport, ILS250). Intensities of the spectrally dispersed WLC probe pulses are monitored by miniature spectrograph (OceanOptics, USB2000+). To obtain the time-resolved transient absorption difference signal (Δ A) at a specific time, the pump pulses were chopped at 25 Hz and absorption spectra intensities were saved alternately with or without pump pulse. Typically, 6000 pulses excite samples to obtain the TA spectra at a particular delay time. The polarization angle between pump and probe beam was set at the magic angle (54.7°) using a Glan-laser polarizer with a half-wave retarder in order to prevent polarization-dependent signals. Cross-correlation fwhm in pump-probe experiments was less than 200 fs and chirp of WLC probe pulses was measured to be 800 fs in the 400-800 nm region. To minimize chirp, all reflection optics in probe beam path and 2 mm path length of quartz cell were used. After fluorescence and TA experiments, we carefully checked absorption spectra of all compounds to avoid artifact from degradation and photo-oxidation of samples. The HPLC grade solvents were used in all steady-state and time-resolved spectroscopic studies. Decay associated spectra were calculated by using an external software (Surface Explorer Pro, Ultrafast Systems) with chirp compensation and singular value deposition method retrieved from the time-resolved TA spectra.

1-3. Quantum Mechanical Calculation

Quantum mechanical calculations were performed with the Gaussian 03 program suite.[S1] All calculations were carried out by the density functional theory (DFT) method with Becke's three-parameter hybrid exchange functionals and the Lee-Yang-Parr correlation functional (B3LYP), employing the 6-31G* basis set. The X-ray crystal structures of **1**, Hückel conformational isomer of **3**, **5**, and **6** were used as initial geometry for geometry optimization without any modification and were used for time dependent density functional theory (TD-DFT) calculations. For, **2**, Möbius conformational isomer of **3**, and **4** the optimized geometry and vertical transitions were virtually calculated based on the X-ray crystal structure of **1** and Huckel conformational isomer of **3**.

1-4. NMR Measurement

^{1}H NMR spectra were recorded on a JEOL ECA-600 spectrometer (600 MHz), using the residual solvent in CD_2Cl_2 and THF-d_8 as the internal reference (δ = 7.26, 5.30, 6.00 and 3.58 ppm respectively).

1-5. X-Ray Crystallography

X-Ray data were taken on a Rigaku RAXIS-RAPID imaging plate diffractometer using a graphite monochromator with $Mo_{K\alpha}$ radiation (λ = 0.71069 Å) at -150 °C. Data collection and reduction were performed using *PROCESS-AUTO* and *CrystalStructure* on a Rigaku program, or *Bruker SMART* and *Bruker SAINT* on a Bruker program. The data were processed and scaled using the program HKL2000 package.[S2] The structures were solved by direct methods (*SIR97*[S3] or *SHELXS97*[S4]), and refined with full-matrix least square technique (*SHELXL97*[S3]) on a Rigaku *CrystalStructure* software package.

2. Variable-Temperature NMR Measurement

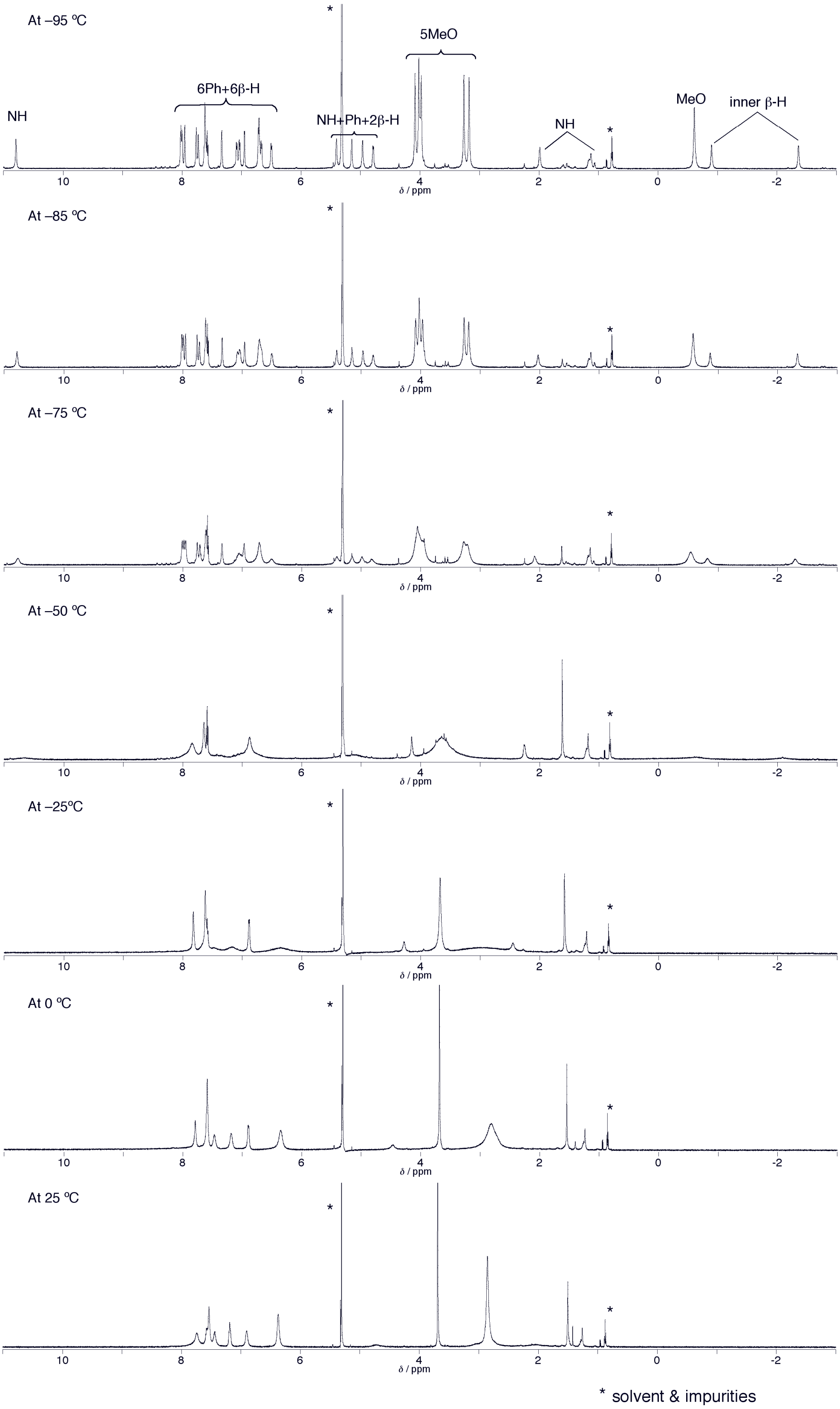

Figure S1. ^{1}H NMR spectra of **2** in CD_2Cl_2 from 25 to -95 ºC.

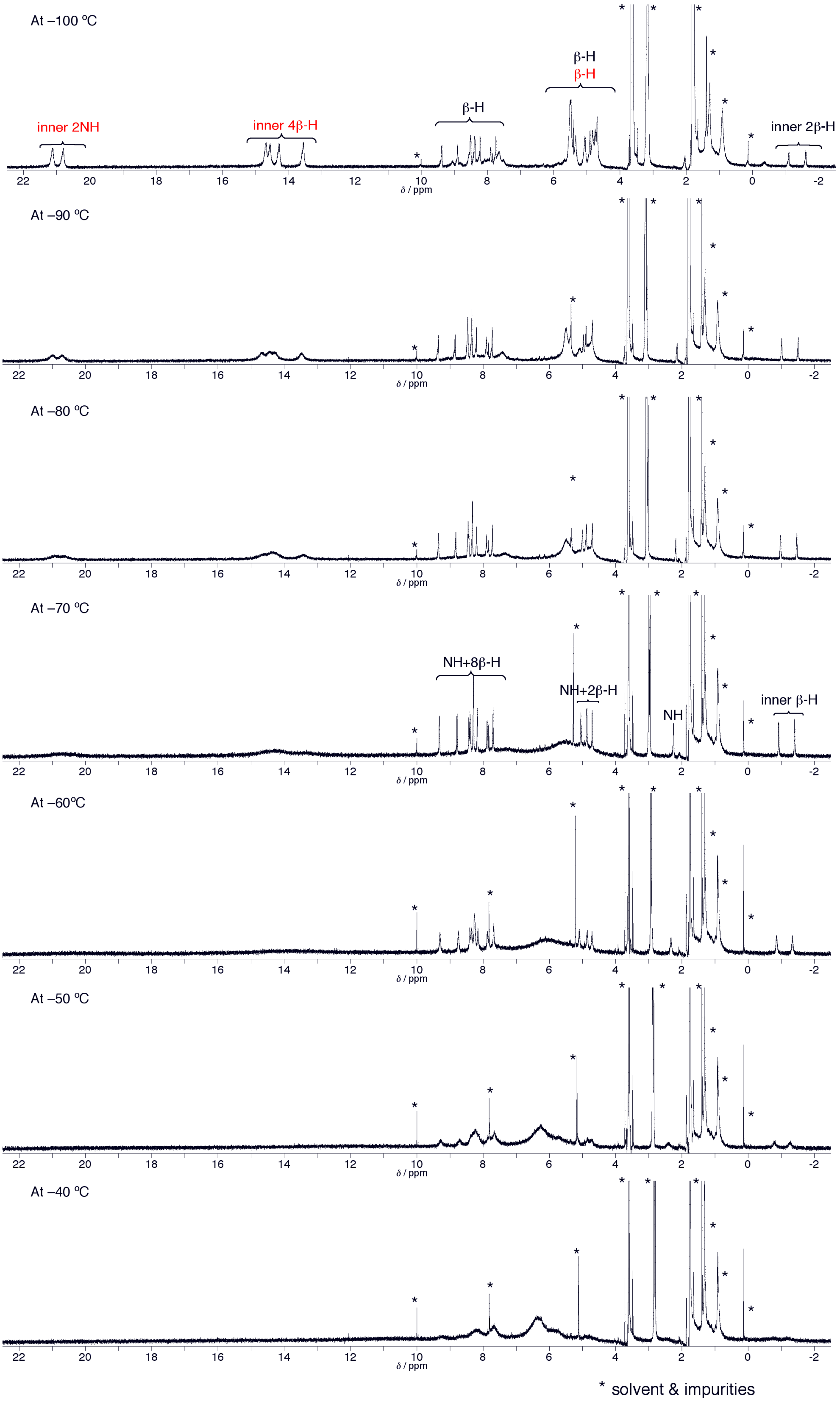
At −100 °C
inner 2NH
inner 4β-H
β-H
β-H
β-H
inner 2β-H
At −90 °C
At −80 °C
At −70 °C
NH+8β-H
NH+2β-H
NH
inner β-H
At −60°C
At −50 °C
At −40 °C
22
20
18
16
14
12
10
8
6
4
2
0
-2
δ / ppm
* solvent & impurities

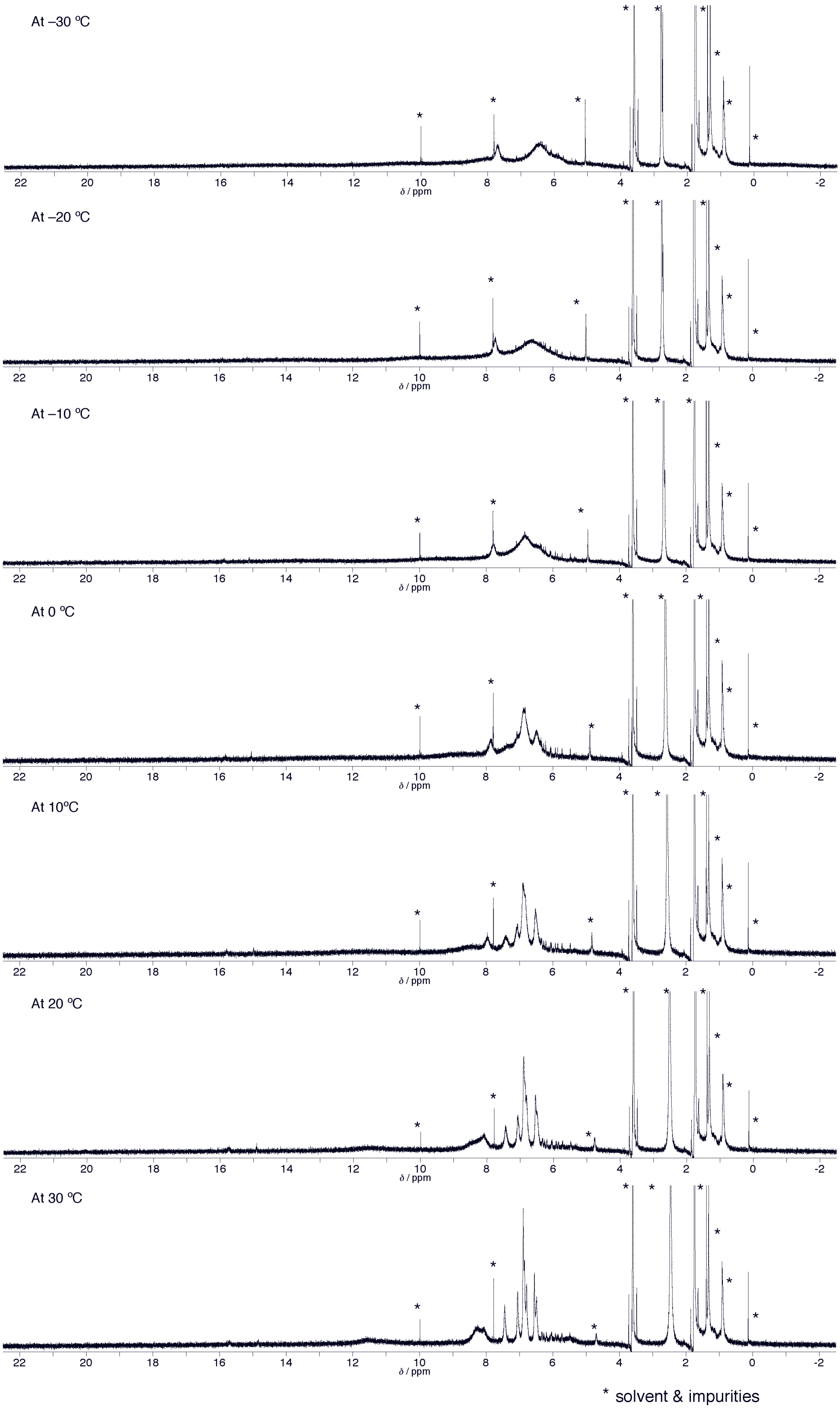

Figure S2. ^{1}H NMR spectra of **3** in THF-d_8 from 30 to -100 ºC. Peaks due to Möbius isomer and Hückel isomer are indicated as black and red, respectively.

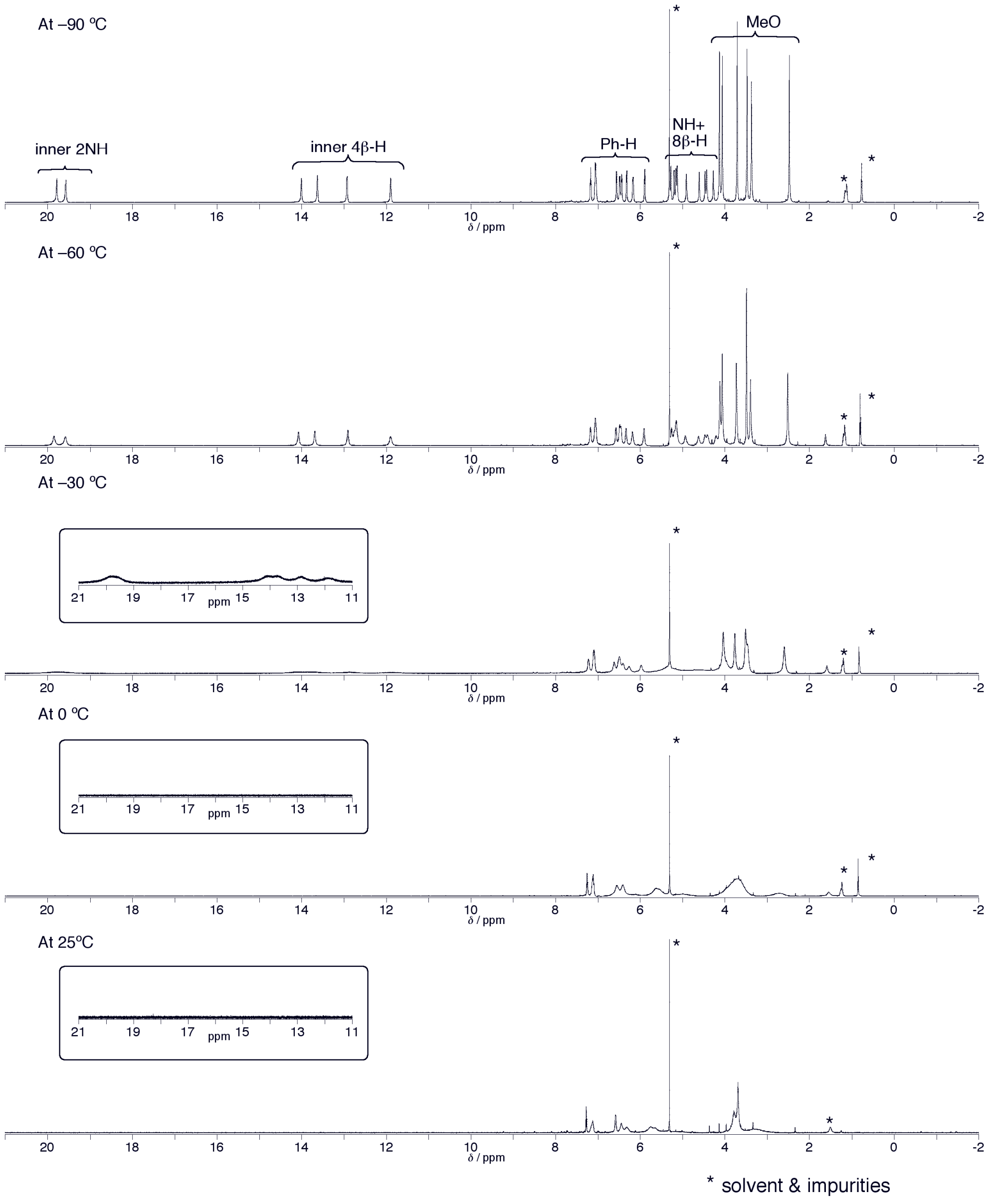

Figure S3. ^{1}H NMR spectra of **4** in THF-d_8 from 25 to -90 ºC.

3. X-Ray Crystallography

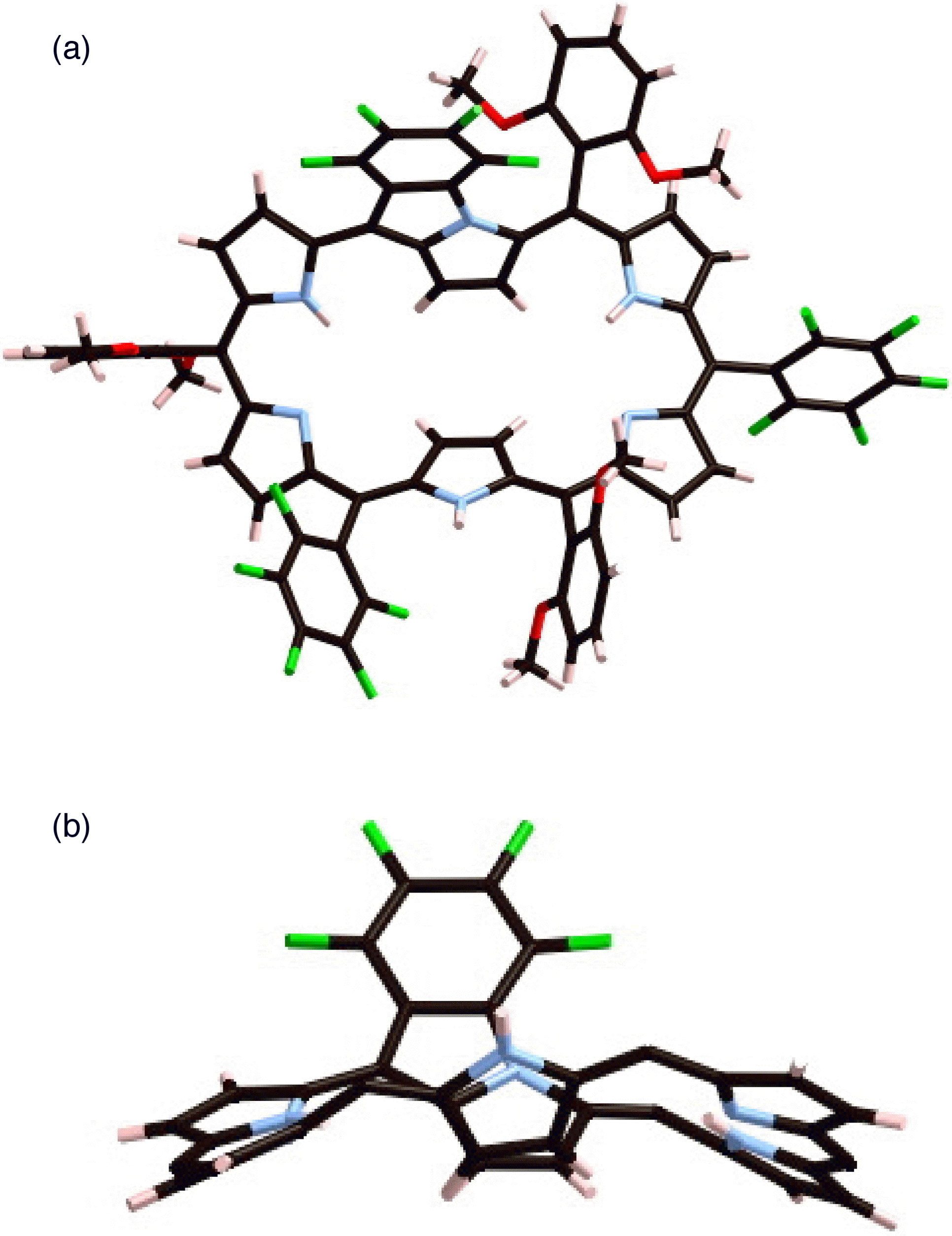

Figure S4. Preliminary X-ray crystal structure of **4**; (a) top view and (b) side view. In the side view, *meso*-substituents were omitted for clarity.

4. Solvent Dependent Absorption Spectra

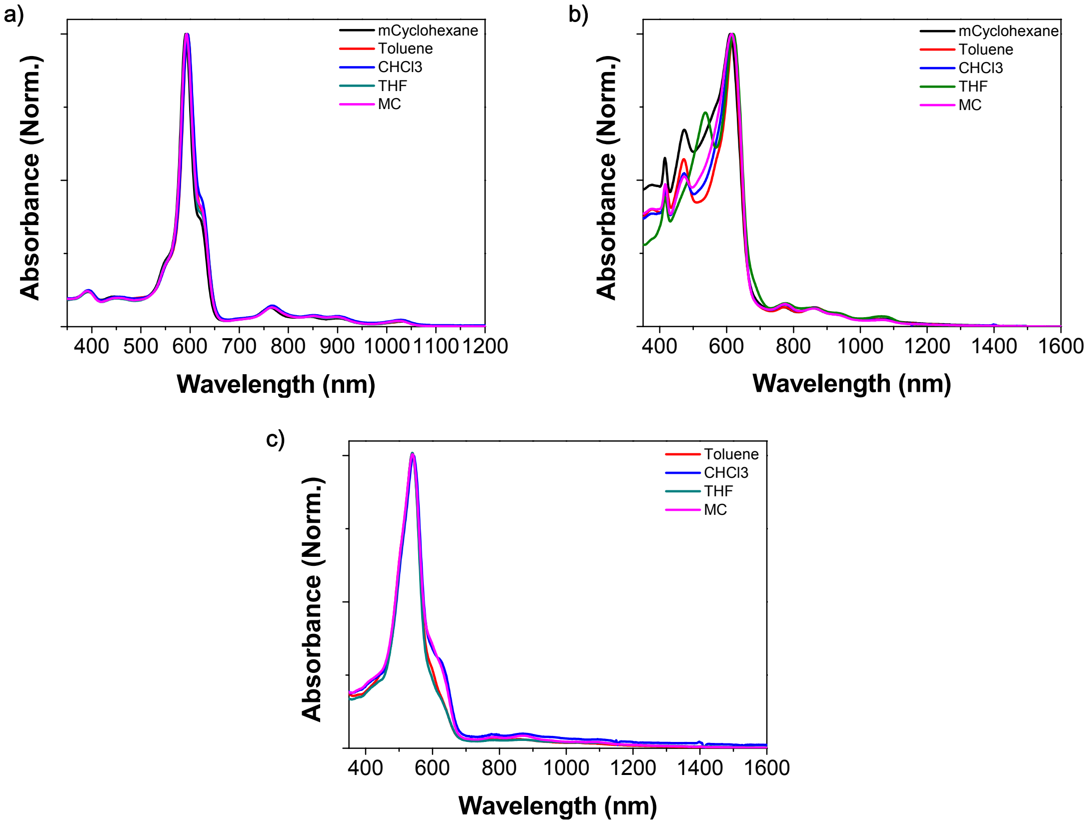

Figure S5. Solvent dependent absorption spectra of [28]hexaphyrin **2** (a), singly fused [28]hexaphyrins **3** (b) and **4** (c).

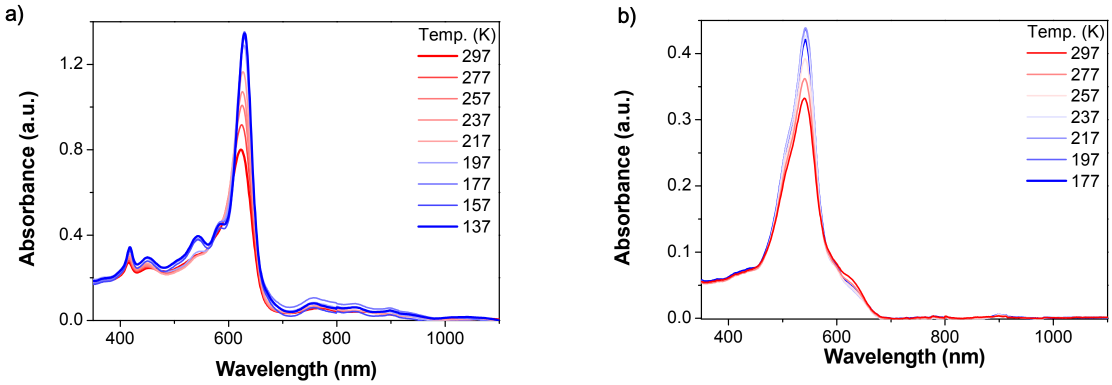

Figure S6. Temperature dependent absorption spectra of singly fused [28]hexaphyrins **3** (a) and **4** (b) in *m*-THF.

5. TD-DFT calculation

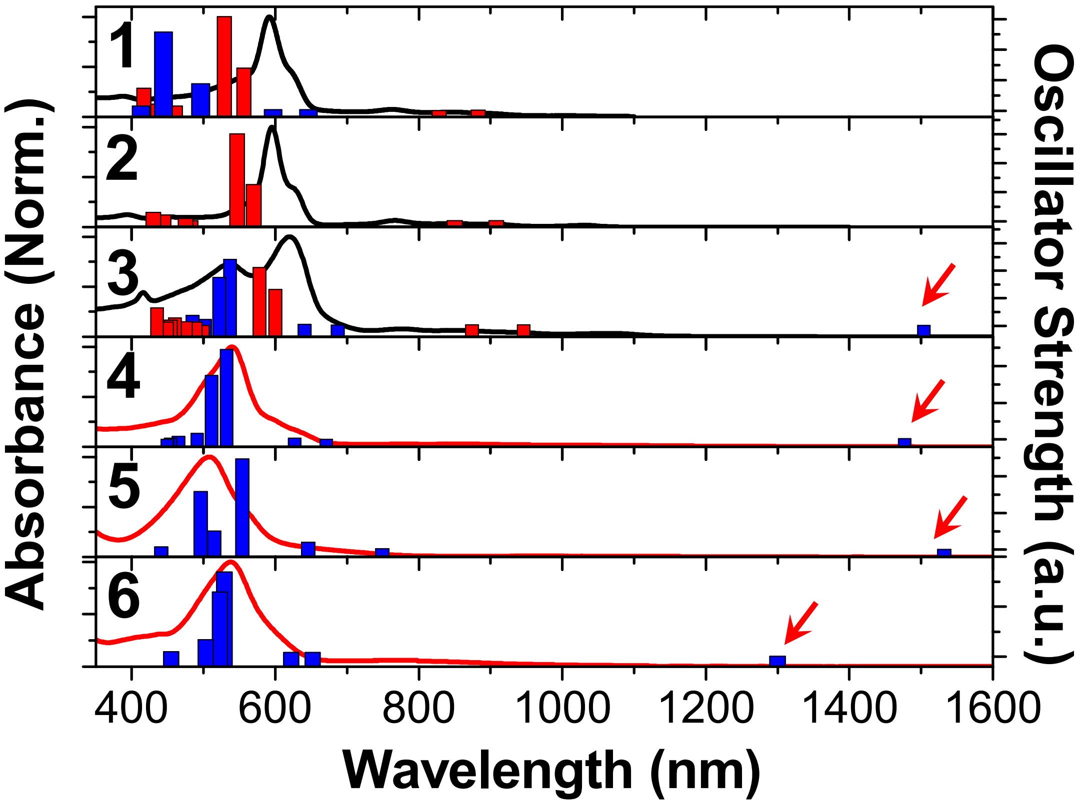

Figure S7. Steady-state absorption spectra and calculated vertical transitions of fused hexaphyrins. The oscillator strengths of singly fused [28]hexaphyrin **3** are calculated based on its two conformational isomers, Möbius aromatic (red columns) and Hückel antiaromatic one (gray columns). Red arrows indicate the optically dark state which are mainly contributed by HOMO-LUMO transition. The calculated energy gaps between HOMO and LUMO are 1.33, 1.36, and 1.44 eV for **4**, **5**, and **6**, respectively.

.

6. fs-Transient Absorption

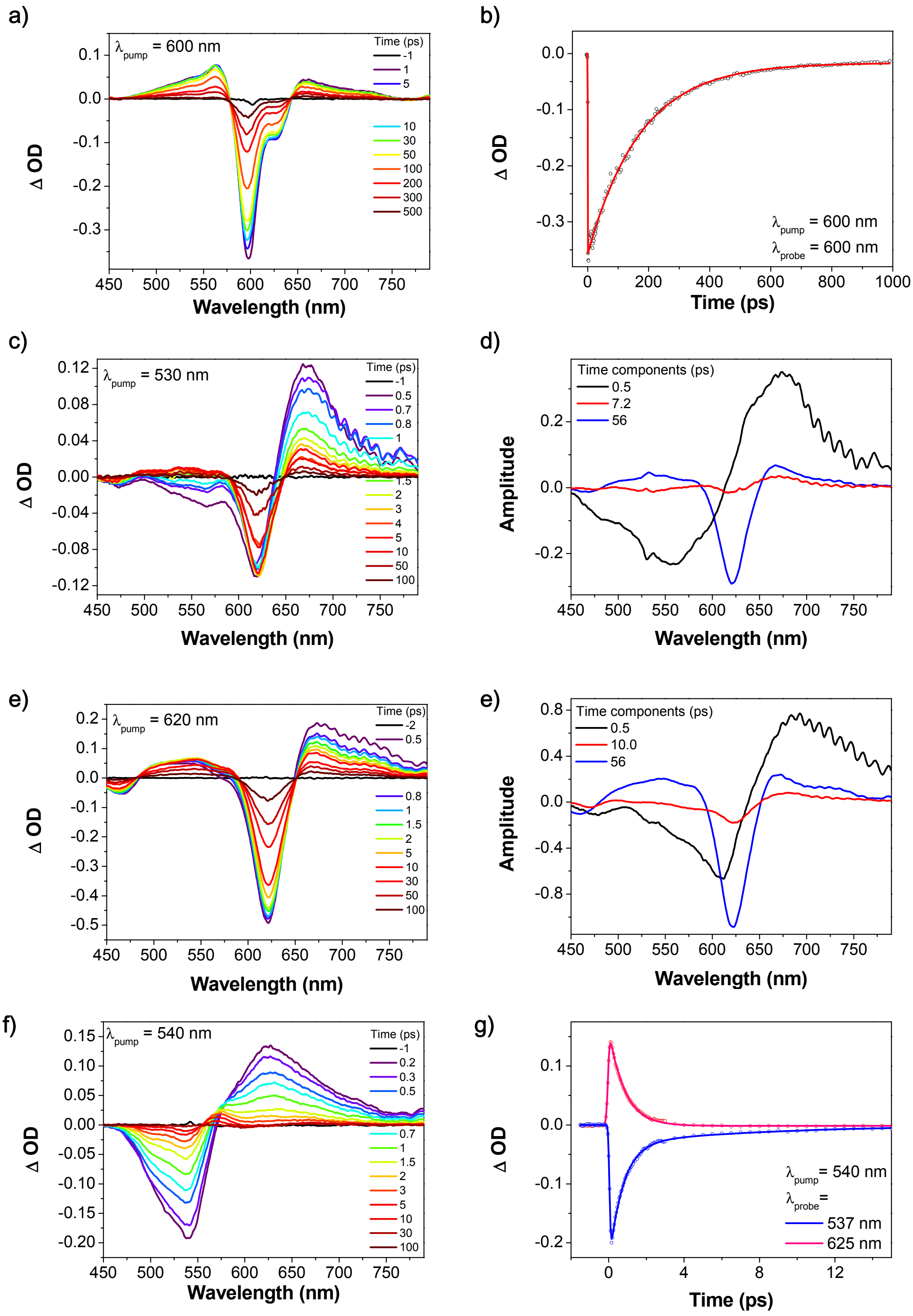

Figure S8. Transient absorption spectra of [28]hexaphyrins **2** (a), **3** (c and e), and **4** (f) in toluene obtained with 600, 530, 620, and 540 nm excitation, respectively. Excited decay profiles for **2** (b) and **4** (g) and decay associated spectra for **3** are presented on the right panels

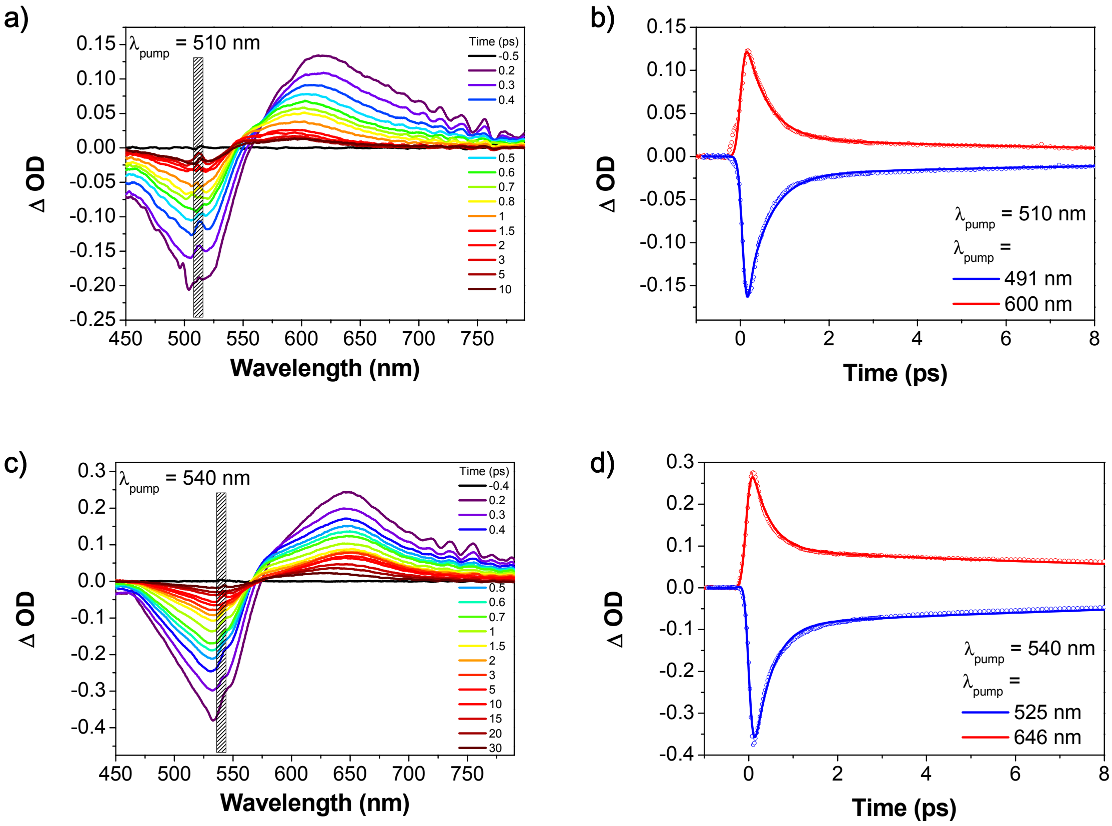

Figure S9. Transient absorption spectra (left) and decay profiles (right) of doubly fused [28]hexaphyrin **5** and **6** in toluene obtained with 510 and 540 nm excitation, respectively.

Table 1. Absorption peak maxima and singlet excited-state time of [28]hexaphyrins.

Molecule	Conformation	Abs (nm)	fs-TA measurement	
			λ_{pump} (nm)	τ_S (ps)
1	Möbius, planar	551, 592, 763, 847, 899, 1017	580	17, 210
			620	183
2	Möbius	552, 595, 767, 849, 899, 1032	590	184
3	Möbius, Planar	472, 617, 771, 864	530	0.9, 12, 73
			620	73
4	Planar (saddle)	540, 850	540	< 1, 6.7
5	Planar	508	510	< 1, 10.5
6	Planar	538, 763	540	< 1, 15.7

7. References

S1. Gaussian 03 (Revision C.02), M. J. Frisch, G. W. Trucks, H. B. Schlegel, G. E. Scuseria, M. A. Robb, J. R. Cheeseman, J. A. Montgomery, Jr., T. Vreven, K. N. Kudin, J. C. Burant, J. M. Millam, S. S. Iyengar, J. Tomasi, V. Barone, B. Mennucci, M. Cossi, G. Scalmani, N. Rega, G. A. Petersson, H. Nakatsuji, M. Hada, M. Ehara, K. Toyota, R. Fukuda, J. Hasegawa, M. Ishida, T. Nakajima, Y. Honda, O. Kitao, H. Nakai, M. Klene, X. Li, J. E. Knox, H. P. Hratchian, J. B. Cross, V. Bakken, C. Adamo, J. Jaramillo, R. Gomperts, R. E. Stratmann, O. Yazyev, A. J. Austin, R. Cammi, C. Pomelli, J. W. Ochterski, P. Y. Ayala, K. Morokuma, G. A. Voth, P. Salvador, J. J. Dannenberg, V. G. Zakrzewski, S. Dapprich, A. D. Daniels, M. C. Strain, O. Farkas, D. K. Malick, A. D. Rabuck, K. Raghavachari, J. B. Foresman, J. V. Ortiz, Q. Cui, A. G. Baboul, S. Clifford, J. Cioslowski, B. B. Stefanov, G. Liu, A. Liashenko, P. Piskorz, I. Komaromi, R. L. Martin, D. J. Fox, T. Keith, M. A. Al-Laham, C. Y. Peng, A. Nanayakkara, M. Challacombe, P. M. W. Gill, B. Johnson, W. Chen, M. W. Wong, C. Gonzalez, and J. A. Pople, Gaussian, Inc., Wallingford CT, **2004**.

S2. Z. Otwinowski, W. Minor, *Methods Enzymol.* **1997**, *276*, 307-326.

S3. *SIR97* : a new tool for crystal structure determination and refinement; A. Altomare, M. C. Burla, M. Camalli, G. L. Cascarano, C. Giacovazzo, A. Guagliardi, A. G. Moliterni, G. Polidori, and R. Spagna, *J. Appl. Cryst.* **1999**, *32*, 115.

S4. G. M. Sheldrick, *SHELXS-97* and *SHELXL-97* (*SHELXH-97*), Program for the solution and refinement of crystal structures, University of Göttingen, Göttingen, Germany, 1997